Spin-dependent Mn X-ray absorption near-edge structure of MnF_2: full multiple-scattering analysis

1994 J. Phys.: Condens. Matter 6 9817

(http://iopscience.iop.org/0953-8984/6/45/030)

J. Phys.: Condens. Matter 6 (1994) 9817–9824. Printed in the UK

Spin-dependent Mn x-ray absorption near-edge structure of MnF_2: full multiple-scattering analysis

A V Soldatov†‖, I E Stekhin†, A P Kovtun‡ and A Bianconi§

† Department of Solid State Physics, Rostov University, Sorge Street 5, Rostov-Don 344104, Russia

‡ Institute of Physics, Rostov University, Stachki 192, Rostov-Don 344104, Russia

§ Dipartimento di Fisica, Università di Roma 'La Sapienza', 00185 Roma, Italy

Received 9 May 1994

Abstract. The self-consistent full multiple-scattering analysis of the spin-dependent Mn K-edge x-ray absorption near-edge structure (XANES) of MnF_2 has been carried out. We succeeded in calculating the spin-dependent XANES over a 40 eV energy range in the continuum above the absorption threshold with the help of a self-consistent spin-polarized method in agreement with experimental data. We show that both the spin-dependent transition matrix element and the Mn p partial density of states contribute to the spin-dependent Mn K-edge XANES of MnF_2.

1. Introduction

The compound MnF_2 has been of interest in this last decade, primarily owing to its magnetic properties. The electronic structure of MnF_2 has been studied both experimentally and theoretically, but mostly without taking into account the spin interactions. X-ray photoemission spectra of MnF_2 [1] have been analysed using the Anderson impurity model to investigate the charge-transfer peculiarities [2]. The x-ray absorption near-edge structure (XANES) of MnF_2 has been measured above the Mn K edge [3, 4], above the F K edge [5] and above the Mn $L_{2,3}$ edge [6]. The multiple-scattering formalism has been applied to the analysis of the F K-edge XANES in MnF_2 [7].

Recently it became possible to study magnetic ordering in solids with the help of magnetic circular x-ray dichroism (MCD) [8–13]. MCD is usually observed in $L_{2,3}$-edge x-ray absorption and the need for sophisticated theoretical treatments has been pointed out [14–18]. MCD has been applied to the study of the systems with ferromagnetic order. It requires a strong external magnetic field for application to paramagnetic systems such as biological molecules. On the contrary it seems to be useless in the case of antiferromagnetic systems.

A new high-resolution spin-dependent XANES technique has been developed recently [19] and its application to MnF_2 [20] has displayed a very pronounced difference in the energy positions and relative intensities of XANES peaks, corresponding to two different spin configurations of the MnF_2 electronic subsystem. The interpretation of the measured spin-dependent XANES data [20] was based on analogy of the Mn Kβ fluorescence spectrum with the Mn 3p x-ray photoemission spectrum. It was shown [21] that even in the case of the Mn 3p x-ray photoemission spectrum there are some difficulties in the accurate interpretation

‖ Author to whom correspondence should be addressed. Email address: Soldatov@xafs.physfac.rnd.su.

0953-8984/94/459817+08$19.50

of all fine details. Our task is the analysis of the very pronounced difference between the 'majority-spin' and the 'minority-spin' Mn K-edge XANES of MnF_2 obtained by Hamalainen *et al* [20]. Here we consider the pure spin-dependent nature of the spectra, i.e. within the assumption that the 'majority-spin' absorption spectrum corresponds to a dipole transition of the photoelectron from a core level to the unoccupied spin-up states of Mn p symmetry in the conduction band of MnF_2, while the 'minority-spin' absorption spectrum corresponds to a transition from the core level to the unoccupied spin-down states of Mn p symmetry.

In the present paper we report the multiple-scattering analysis of spin-dependent Mn XANES in MnF_2. The full multiple-scattering analysis has been applied to interpret a large number of XANESs in various materials, including the F K-edge XANES of MnF_2 [7] (see, for a review, [22]), but no multiple-scattering calculations in real space devoted to spin-dependent XANES have been carried out until now. Very recently, when most of the present study had been done, a spin-dependent linearized augmented plane-wave (LAPW) study of the MnF_2 band structure in the low-temperature antiferromagnetic phase was reported [23]. The comparison of the spin-dependent Mn p symmetry density of states with the experimental XANES data of Hamalainen *et al* shows general qualitative agreement in the energy positions of the main peaks, but within the assumption of constant dipole transition matrix element it was not possible to obtain agreement in the relative intensity of the low-energy peaks. Another possible reason for this existing disagreement between experimental XANES data of Hamalainen *et al* and the theoretical LAPW results [23] lies in the fact that the experimental spectra were measured at room temperature, where MnF_2 has a simple rutile-type structure, while calculations have been done for the low-temperature antiferromagnetic crystal phase of MnF_2 (although the unit-cell parameters are nearly the same).

2. Method of calculation

It is now well known that the XANES above the K edge of solid matter is generated by the multiple scattering of the excited photoelectron within a cluster (i.e. a group of atoms around an absorbing atom) of a large size consisting of five or even more shells of atoms [22]. On the other hand it is very time consuming to perform a self-consistent spin-dependent calculation within such a large cluster. Therefore we divided our task into two parts: first we obtained in a self-consistent mode two sets of spin-dependent potentials, and second we performed a full multiple-scattering calculation within a large cluster using the calculation method [22] appropriate for continuum states.

In order to obtain two sets of potentials for both spin-up and spin-down configurations we performed a self-consistent spin-resolved calculation of a small cluster MnF_2F_4 that is a fragment of the MnF_2 crystal. The method that we used is based on the self-consistent field scattered waves (SCF $X\alpha$-SW) technique with the Slater $X\alpha$ local density approximation (LDA) [24, 25]. Our approach is close to standard Johnson and Smith [26] technique. We described it previously [27] and its results are found to be in good agreement with experimental data for tantulum and uranium oxides [27, 28]. According to Hund's rule, we assumed that all five Mn 3d electrons are 'spin up', while all Mn 3d 'spin-down' orbitals are unoccupied. The charge of the $MnF_2F_4^{4-}$ cluster has been chosen on the basis of the formal valencies of Mn and F ions. According to the Slater [25] prescription the stabilizing charge ($+4e$) has been distributed over the Watson sphere surface. In order to eliminate the 'extra' electronic levels arising from the additional electrons on the Watson sphere, we used an additional constant potential of 13.6 eV, which leads only to a total shift in the energy scale. This additional lowering of the potential by a constant value leads to the separation

of cluster occupied states from the states localized in the region out of the Watson sphere. These 'false' states are not the results of real interaction between Mn and F states within the cluster but appear as a result of the cluster model itself. These levels can lead to an unphysical Mn 3d charge transfer from the cluster region to the region out of the Watson sphere and make it difficult to reach self-consistency. The cluster has D_{2h} symmetry with a central Mn atom and with Mn–F distances equal to 2.102 Å for the first shell of F atoms and to 2.132 Å for the second shell. According to our procedure of muffin-tin potential construction [29] we have obtained the following values of muffin-tin radii: 1.21 Å for the Mn and 0.90 Å for the F site. The muffin-tin constants are equal to −19.53 eV for the 'spin-up' configuration, and −19.45 eV for the 'spin-down' configuration, if the origin of the energy scale is at the vacuum level. We used the exchange–correlation potential in the Slater form with the exchange–correlation constant $\alpha = 1.0$. We took into account the spherical harmonics with angular momentum $l = 0, 1$ for fluorine spheres and $l = 0, 1, 2$ for the manganese sphere. The criterion of convergency of the self-consistency process was the inequality

$$\max |\rho_\alpha^{i+1}(r) - \rho_\alpha^i(r)| \leqslant 0.001 \tag{1}$$

where i is the number of iterations, $\rho(r)$ is the electronic density and α is the type of spin.

Within the dipole approximation the x-ray absorption coefficient $\alpha(E)$ for the K edge is proportional to both the partial density of unoccupied Mn p symmetry states and the squared dipole transition matrix element, i.e.

$$\alpha(E) \sim |m_L(E)|^2 N_p^{Mn}(E) \tag{2}$$

where $N_p^{Mn}(E)$ is the partial density of unoccupied Mn p symmetry states and

$$m_L(E) = \left(\int \mathrm{d}r\ \Phi_l(r, E)\Delta(r)\Psi_K(r)\right) \Big/ \left(\int \mathrm{d}r\ \Phi_l(r, E)\right)^{1/2} \tag{3}$$

is a normalized dipole transition matrix element, where $\Phi_l(r, E)$ is a solution of the radial Schrödinger equation at energy E for the muffin-tin potential ($l = 1$ for the K edge), $\Delta(r)$ is the electron–photon interaction operator and $\Psi_K(r)$ is a Mn core K-level wavefunction.

Two sets of potentials, corresponding to two different spin states, obtained in the spin-polarized self-consistent calculation of the small $MnF_2F_4^{4-}$ cluster, were used to calculate two sets of partial phase shifts of the photoelectron scattering on these potentials and two dipole transition matrix elements. Then we performed a full multiple-scattering XANES calculation in real space for a sufficiently large cluster in the same manner as in our previous work [30–32], where we did not include the effect of spin-dependent XANES. The algorithm of the full multiple-scattering method, which we have used, was described earlier [22, 33]. For the calculation we consider the rutile structure of MnF_2 crystal [34] (table 1). The cluster of neighbouring atoms around a central Mn is divided into five shells as reported in table 2. In our calculation we included phase shifts with an orbital momentum of up to four, but even for $l = 3$ there are almost no changes in the spectra in comparison with $l = 2$.

3. Results and discussion

In figure 1 we present a schematic diagram of the process resulting in spin-dependent absorption of x-ray photons with energy $h\nu$ involving a dipole transition of the electron

Table 1. Structural parameters (from [34]) for the MnF_2 unit cell used in this paper ($a = b =$ 4.8734 Å; c = 3.3099 Å).

Type of atom	Coordinates in units of *a*, *b*, *c* basis vectors		
	x	*y*	*z*
Mn	0.0	0.0	0.0
Mn	0.5	0.5	0.5
F	0.305	0.305	0.0
F	0.805	0.195	0.5
F	0.695	0.695	0.0
F	0.195	0.805	0.5

Table 2. Structure of the five-shell cluster for MnF_2.

Number of shell	Type of atom	Number of atoms in shell	Number of atoms in cluster	Sphere radii (Å)
1	F	2	3	2.102
2	F	4	7	2.132
3	Mn	2	9	3.309
4	F	4	13	3.699
5	Mn	8	21	3.823

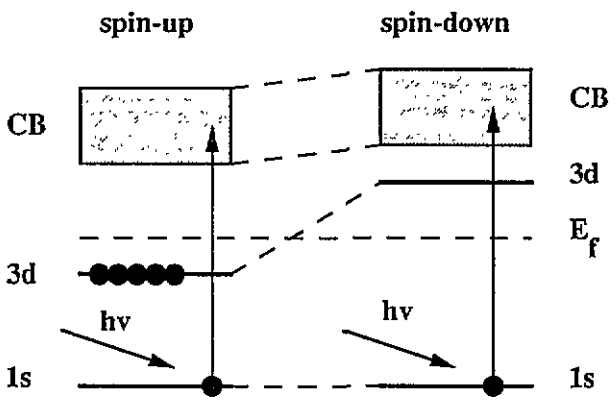

Figure 1. A model of the process resulting in the spin-dependent absorption of an x-ray photon with energy $h\nu$ involving the dipole transition of the electron from core Mn 1s (in spectroscopic notation K) level to the p symmetry states in the conduction band (CB). Mn 3d states are shown in order to stress the difference between the occupation numbers for spin-up and spin-down states. The horizontal broken line indicates the Fermi energy.

from the core Mn 1s (in spectroscopic notation K) level to the p symmetry states in the conduction band. There we show also the levels of Mn 3d passive electrons in order to stress the difference between the occupation numbers for spin-up and spin-down states which lead (mostly through the exchange–correlation potential) to the relative energy shift of the spin-up and spin-down states.

The difference between the potentials corresponding to the two spin configurations is not very large for the Mn site and is almost negligible for the F site. However, the difference between the phase shifts of the scattered photoelectron calculated for these potentials is

significant. The resonant scattering for spin-up d electrons occurs in the energy interval below the Fermi energy, and for spin-down d electrons it occurs above E_F. For electrons with another type of symmetry (s, p and f) the effect of different spin configurations on the phase shifts is not so strong as for the d channel, but their variations will be important for the spin-dependent XANES.

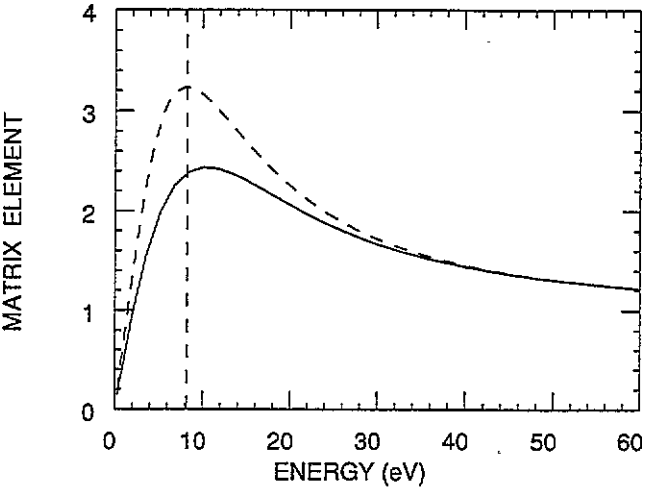

Figure 2. Energy-dependent squared dipole transition matrix elements, corresponding to dipole Mn 1s $\rightarrow$ ϵp electronic transition in MnF_2 for two spin configurations (----, 'spin up'; ——, 'spin down'). The vertical broken line indicates the Fermi energy position.

Another factor (apart from phase shifts and the cluster local structure) which determines the XANES in the multiple-scattering formalism is the transition matrix element (3) which influences the relative intensities of XANES features. In figure 2 we present the squared dipole transition matrix element $|m_L(E)|^2$ as a function of energy for both spin configurations in order to emphasize the importance of this element for the correct description of XANES. As one can see in the energy interval close to the absorption threshold the dipole transition matrix element has a rather significant energy dependence and cannot be treated as a constant (as was done in [23]).

The important step in the multiple-scattering analysis of XANES data is the determination of the size of a cluster of neighbouring atoms around the absorbing Mn atom. The analysis of the dependence of main structures in the XANES on the cluster size shows that convergence with cluster size is reached for a five-shell cluster; therefore all the subsequent spin-dependent XANES calculations were performed using this cluster.

In order to perform a direct comparison with experimental data, one must take into account two factors: the filling of occupied states following the Fermi distribution and the broadening of experimental spectra according to three factors, namely the core hole lifetime, the finite mean free path of the photoelectron and the experimental resolution. We have used a value of 0.7 eV [35] for the K core hole bandwidth, we have taken the energy-dependent function obtained in [36] for the mean free path of the photoelectron and we have used a value of 0.5 eV for the experimental energy resolution. We treated all these factors as contributing to the imaginary part of the self-energy that we use. We reported our theoretical results in the form of the normalized absorption coefficient (i.e. the absorption coefficient

in relative units of atomic absorption α_0 at high energies). So, if one needs to obtain the absolute values of the absorption coefficient, it is possible to do so by multiplying these normalized data by the corresponding value of the atomic absorption jump.

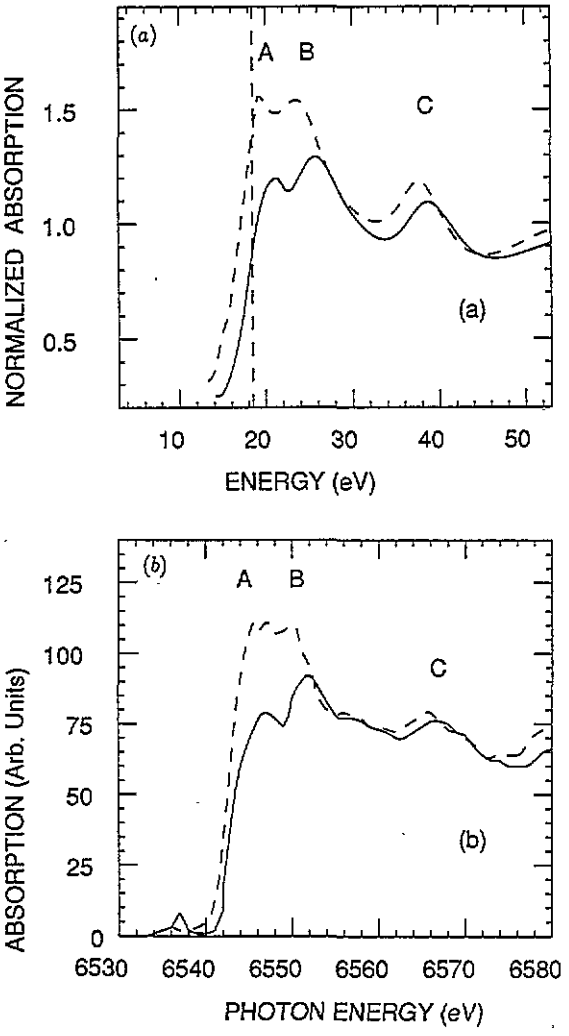

Figure 3. (*a*) Calculated Mn K-edge XANES of MnF_2 for two spin configurations (----, 'spin up'; ——, 'spin down'). The vertical broken line indicates the muffin-tin zero (V_i) positions. (*b*) Experimental spin-dependent XANES spectrum at the Mn K edge in MnF_2 from [20].

In figure 3 we present the results of the theoretical calculation for both spin configurations together with the experimental spin-dependent XANES from [20]. We have found that our calculation correctly predicts the overall shift of the spin-up XANES spectrum towards the low energies, as occurs in the experimental spin-dependent spectra. It shows that the spin-dependent scattering of the photoelectron in the final state of the p electron is at the origin of the spin-dependent XANES of MnF_2 (the same effect that we expected in the EXAFS region of x-ray absorption).

The analysis of the energy positions of the corresponding maxima in the calculated and experimental spectra shows rather good correspondence in the relative positions of the main XANES features for both spin configurations, taking into account the possible value of the accuracy of identification of peak positions. (We did not include the pre-edge peak position determination in this study because the x-ray core hole potential effects on the localized 3d electronic states are stronger than on the itinerant p states. Therefore we cannot treat the pre-edge spectra without taking into account the core hole effect [37].)

4. Conclusions

We have applied spin-polarized SCF full multiple-scattering schemes for the theoretical analysis of continuum states in spin-dependent XANES of MnF_2. Within this method we succeed in obtaining the spin-dependent theoretical XANES above the Mn K edge of MnF_2 which is in agreement with the experimental data of Hamalainen *et al.* To our knowledge this is the first time that the spin-dependent multiple-scattering approach has been reported for continuum delocalized states. We think that this method will be effective for the theoretical analysis of spin-dependent x-ray absorption in complex and disordered matter, where other approaches using band-structure theory [14, 23] cannot be used. Our approach can be easily applied to the theoretical analysis of spin-dependent extended x-ray absorption fine structure, while band calculations using k-space representation (e.g. LAWP type [23]) show poor convergency and became too time consuming in high-energy regions.

Acknowledgments

This research was partially supported by the NATO Scientific Division (grant CRG 930305) and the Ministry of Science and Higher Education of Russia. One of us (AVS) would like to acknowledge the kind hospitality of Rome University 'La Sapienza' where this research was partially carried out.

References

[1] Frost D C, McDowell C A and Woolsey I S 1972 *Chem. Phys. Lett.* **17** 320
[2] Park J, Ryu S, Han M-S and Oh S-J 1988 *Phys. Rev.* B **37** 10867
[3] Rao B J and Chetal A R 1983 *J. Phys. Chem. Solids* **44** 677
[4] Sinha S H and Chetal A R 1987 *Phys. Status Solidi* b **143** 595
[5] Nakai S, Kawata A, Ohashi M, Kitamura M, Sigiura C and Mitsuishi T 1988 *Phys. Rev.* B **37** 10895
[6] Nakai S, Ogata K, Ohashi M, Sugiura C, Mitsuishi T and Maezawa H 1985 *J. Phys. Soc. Japan* **54** 4034
[7] Yamasaki K, Fujikawa T and Nakai S 1989 *J. Phys. Soc. Japan* **58** 2962
[8] *Schutz G, Wagner W, Wilhelm W, Kienle P, Zeller R, Frahm R and Materlick G 1987 Phys. Rev. Lett. 58* 737
[9] Schutz, Knulle M, Wienke R, Wagner W, Wilhelm W, Kienle P and Frahm R 1988 *Z. Phys.* B **73** 67
[10] Chen C T, Sette F, Ma Y and Modesti S 1990 *Phys. Rev.* B **42** 7262
[11] Rudolf P, Sette F, Tjeng L H, Meigs G and Chen C T 1991 *J. Appl. Phys.* **70** 6338
[12] Baudelet F, Dartyge E, Fontaine A, Brouder Ch, Krill G, Kappler J P and Piecuch M 1991 *Phys. Rev.* B **43** 5857
[13] Giorgetti C, Pizzini S, Dartyge E, Fontaine A, Bauder F, Bauer Ph, Krill G, Miraglia S, Fruchart D and Kappler J P 1993 *Phys. Rev.* B **48** 12 732
[14] Ebert H, Dritter B, Zeller R and Schutz G 1989 *Solid State Commun.* **69** 485
[15] Carra P and Altarelli M 1990 *Phys. Rev. Lett.* **64** 1286

[16] Imada S and Jo T 1990 *J. Phys. Soc. Japan* **59** 3358
[17] Thole B T, Carra P, Sette F and van der Laan G 1992 *Phys. Rev. Lett.* **68** 1943
[18] Jo T and Sawatzky G A 1991 *Phys. Rev.* B **43** 8771
[19] Hamalainen K, Siddons D P, Hastings J B and Berman L E 1991 *Phys. Rev. Lett.* **67** 2850
[20] Hamalainen K, Kao C-C, Hastings J B, Siddons D P, Berman L E, Stojanoff V and Cramer S P 1992 *Phys. Rev.* B **46** 14274
[21] Hermsmeier B D, Fadley C S, Sinkovic B, Krause M O, Jimenrz-Mier J, Gerard P, Carlson T A, Manson S T and Bhattacharya S K 1993 *Phys. Rev.* B **48** 12425
[22] Durham P J 1989 *X ray Absorption: Principles, Applications and Techniques of EXAFS, SEXAFS and XANES* (New York: Wiley) p 53
[23] Dufek P, Schwarz K and Blaha P 1993 *Phys. Rev.* B **48** 12672
[24] Hohenberg P and Kohn W 1964 *Phys. Rev.* **136** 864
[25] Slater J C 1965 *J. Chem. Phys. Suppl.* **43** 228
[26] Johnson K H and Smith F C 1972 *Phys. Rev.* B **5** 831
[27] Gubskii A L, Kovtun A P and Khanin S D 1987 *Sov. Phys.–Solid State* **29** 611
[28] Teterin Yu A, Baev A S, Vedrinsky R V, Gubsky A L, Zelenkov A G and Kovtun A P 1981 *Sov. Phys.–Dokl.* **26** 67
[29] Li C, Pompa M, Congiu-Castellano A, Della Longa S and Bianconi A 1990 *Physica* C **175** 369
[30] Soldatov A V, Della Longa S and Bianconi A 1993 *Phys. Rev.* B **47** 16155
[31] Soldatov A V, Della Longa S and Bianconi A 1993 *Solid State Commun.* **85** 863
[32] Soldatov A V, Ivanchenko T S, Stekhin I E and Bianconi A 1993 *J. Phys.: Condens. Matter* **5** 7521
[33] Vvedensky D D, Saldin D K and Pendry J B 1986 *Comput. Phys. Commun.* **40** 421
[34] Wyckoff R W G 1963 *Crystal Structures* (New York: Interscience)
[35] Keski-Rahkonen O and Krause M O 1974 *At. Data Nucl. Data Tables* **14** 139
[36] Muller J E, Jepsen O and Wilkins J W 1982 *Solid State Commun.* **42** 365
[37] Bianconi A 1989 *X ray Absorption: Principles, Applications and Techniques of EXAFS, SEXAFS and XANES* (New York: Wiley) p 537